$$\int_0^\infty xe^{-x}L_{p-1}L_p\,dx = -p$$

$$\int_0^\infty x^2e^{-x}L_pL_p\,dx = 6p^2 + 6p + 2$$

$$\int_0^\infty x^2e^{-x}L_{p-1}L_p\,dx = -4p^2$$

$$\int_0^\infty x^2e^{-x}L_{p-2}L_p\,dx = p(p-1).$$

ACKNOWLEDGMENT

The author would like to acknowledge the contributions of others to the research reported here. The mirrors were machined by W. Polzin; G. Rasmussen designed circuits and patiently took measurements; and J. D. Zook freely discussed various aspects of perturbation theory.

REFERENCES

[1] A. L. Schawlow and C. H. Townes, "Infrared and optical masers," *Phys. Rev.*, vol. 29, pp. 1940–1949, Dec. 1958.
[2] G. Goubau and F. Schwering, "On the guided propagation of electromagnetic wave beams," *IRE Trans. Antennas Propagat.*, vol. AP-9, pp. 248–256, May 1961.
[3] A. G. Fox and T. Li, "Resonant modes in a maser interferometer," *Bell Syst. Tech. J.*, vol. 40, pp. 453–488, Mar. 1961.
[4] G. D. Boyd and J. P. Gordon, "Confocal multimode resonator for millimeter through optical wavelength masers," *Bell Syst. Tech. J.*, vol. 40, pp. 489–508, Mar. 1961.
[5] G. D. Boyd and H. Kogelnik, "Generalized confocal resonator theory," *Bell Syst. Tech. J.*, vol. 41, pp. 1347–1369, July 1962.
[6] P. F. Checacci and A. M. Scheggi, "Microwave models of optical resonators," *Appl. Opt.*, vol. 4, pp. 1529–1533, Dec. 1965.
[7] H. Kogelnik and T. Li, "Laser beams and resonators," *Appl. Opt.*, vol. 5, pp. 1550–1567, Oct. 1966.
[8] R. W. Zimmerer, "Spherical mirror Fabry-Perot resonators," *IEEE Trans. Microwave Theory Tech.*, vol. MTT-11, pp. 371–379, Sept. 1963.
[9] G. Sansone, *Orthogonal Functions*. New York: Interscience, 1959, ch. IV.

A Unified Variational Solution to Microstrip Array Problems

VITTORIO RIZZOLI

***Abstract*—A very general variational procedure is used to compute single or coupled microstrips under the quasi-TEM approximation. The capacitance model is found by means of a unique fundamental cell. The method is essentially an extension of Smith's [1], but may be used to study a wider variety of problems, such as nonuniform strip arrays, coplanar striplines, and broad-side coupled strips. Moreover, it is also possible to compute the coupling capacitance between nonadjacent strips.**

I. INTRODUCTION

IT has been shown in [1], [2], that the capacitance model of single or coupled microstrip lines can be computed when capacitances of suitable "fundamental cells" are known. A fundamental cell is a single-strip rectangular region bounded by electric and/or magnetic walls. In [1] uniform strip arrays are computed by means of two fundamental cells, while in [2] the procedure is extended to nonuniform arrays by use of three fundamental cells. In the present paper a unique fundamental cell is used, including all the different types as special cases. In this way the computation procedure is unified and becomes particularly suitable for programming on a digital computer. Coplanar striplines as well as broad-side coupled strips can be calculated by this method; the saving in computer time is high (up to 70 percent) with respect to techniques based on optimization of the charge distribution, such as [7], and even higher with respect to relaxation techniques, such as [6]. This is due to the use of a variational method in the computations. The method is also suitable for computing the coupling capacitance between nonadjacent strips of a coplanar array.

Manuscript received May 5, 1974; revised September 16, 1974. This work was sponsored by the Italian National Research Council (CNR).
The author is with the Istituto di Elettronica, Università di Bologna, Bologna, Italy.

II. CAPACITANCE CALCULATION FOR A RECTANGULAR CELL

The fundamental cell that will be referred to throughout this paper is shown in Fig. 1. Magnetic and electric walls are represented by dashed and full lines, respectively, while a dotted and dashed line may represent either type of wall. In Fig. 1, $w_1(w_2)$ is understood to be zero when the left (right) wall is magnetic. Zero thickness conductors are assumed.

Now suppose that the center strip is held at a 1-V potential while the two side strips are grounded. Then a lower bound on the capacitance C of the center strip with respect to ground may be found by the variational series [2]:

$$\frac{1}{C} = \frac{u}{\epsilon_0 a_0/g_2 + \epsilon_0 a_0/(g_1 + d_1/\epsilon_r)} + \frac{a_0}{2Q^2}\sum_n^{\infty} f_n \rho_n^2 \quad (1)$$

where

$$f_n = \frac{l}{n\pi\epsilon_0} \cdot \frac{\tanh(n\pi g_2/l)[\tanh(n\pi d_1/l) + \tanh(n\pi g_1/l)\epsilon_r]}{\tanh(n\pi g_2/l)[1 + \epsilon_r \tanh(n\pi g_1/l)\tanh(n\pi d_1/l)]\epsilon_r + \tanh(n\pi d_1/l) + \epsilon_r \tanh(n\pi g_1/l)}. \quad (2)$$

In (1), Q represents the total charge on the center strip, and ρ_n is the nth coefficient of the Fourier expansion of the line charge density $\rho(x)$ at the upper air-dielectric interface (i.e., for $y = g_1 + d_1$). In order to compute ρ_n when w_1 and/or w_2 is nonzero, the negative charge on the side strips must be taken into account.

Equations (1) and (2) are so written as to include all the possible cases; the parameters l and u in them must be specified according to the type of side walls. The same is true for the following expression of the coefficient ρ_n:

$$\rho_n = \frac{2}{a_0}\int_{-a_0/2}^{a_0/2} \rho(x) \sin[n(\pi x/l + \phi) + \theta]\, dx. \quad (3)$$

The different values of the parameters u,l,ϕ,θ are best expressed in terms of two indexes, I_1 and I_2, whose values are bound to the type of side walls in the way shown in Table I.

When I_1 and I_2 are given the values specified in Table I, we have

$$l = (1 + |I_2 - I_1|)a_0$$

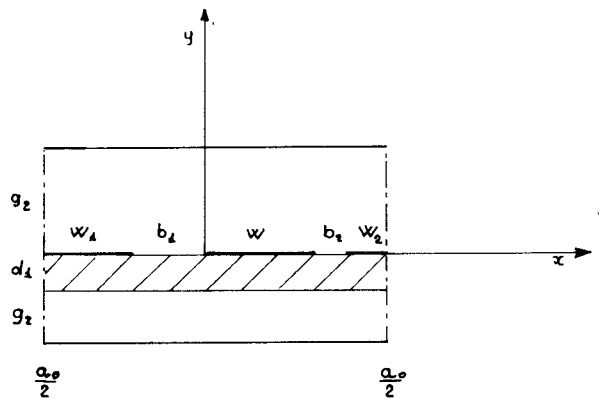

Fig. 1. Basic rectangular cell.

TABLE I

value of I_1	type of left wall	value of I_2	type of right wall
1	electric	1	electric
2	magnetic	2	magnetic

$$\phi = \frac{\pi}{2(1 + |I_2 - I_1|)}$$

$$\theta = (I_1 - 1)\tfrac{1}{2}\pi$$

$$u = (I_1 - 1)(I_2 - 1). \quad (4)$$

Finally, the increment of the summation variable n is given by

$$\Delta n = 1 + |I_2 - I_1|. \quad (5)$$

This formulation, although somewhat cumbersome, is very useful in view of the automatic computation of the capacitance.

In practical cases, a trial function is used to calculate the coefficients ρ_n and the total charge Q. Since the expression (1) is stationary with respect to $\rho(x)$, a good approximation can be achieved even by a poor choice of the trial function. Here, the trial function will be chosen as the effective charge density for a homogeneous symmetrical cell having height $2h_0$ as shown in Fig. 2. h_0 is defined as

$$h_0 = \min(g_1 + d_1, g_2) \quad (6)$$

so that a good trial function is found even in the case of inverted microstrips.

If the capacitance of this cell is denoted by C_0, then from (1) we can obtain the series:

$$\frac{1}{C} = \frac{2}{(\epsilon_r + 1)C_0} + u\left[\left(\frac{\epsilon_0 a_0}{g_2} + \frac{\epsilon_0 a_0}{g_1 + d_1/\epsilon_r}\right)^{-1} - \frac{h_0}{(\epsilon_r + 1)\epsilon_0 a_0}\right] + \frac{a_0}{2C_0^2}\sum_n^{\infty}\left(f_n - \frac{2}{\epsilon_r + 1} f_{n0}\right)\rho_n^2 \quad (7)$$

where

$$f_{n0} = \frac{l}{2n\pi\epsilon_0}\tanh\frac{n\pi h_0}{l}. \quad (8)$$

Equation (7) is Smith's series for C; it is much more rapidly converging than (1) since its nth term decays exponentially with increasing n for large values of n. In most practical cases the capacitance in air C_1 is also required. This is simply obtained by putting $\epsilon_r = 1$ in (2) and (7). Note that the same trial function, i.e., the same coefficients ρ_n, may be used in the two cases so that C and C_1 may be computed simultaneously with a negligible increase of computer time.

An upper bound on the value of C may be easily found

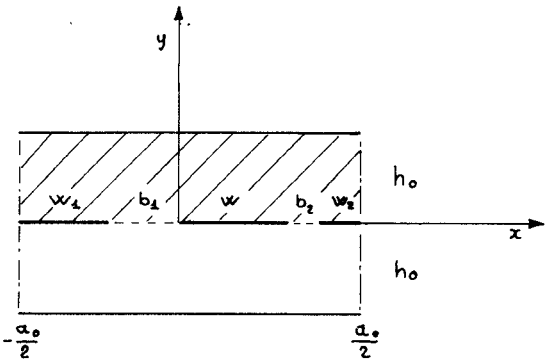

Fig. 2. Homogeneous symmetrical cell for trial function calculations.

as well. In fact, it should be noted that (1) holds exactly when the coefficients ρ_n and the total charge Q are computed by means of the true charge-distribution function $\rho(x)$. In this case $Q = C$ since the voltage is unity. Now if we denote by $\psi(x)$ the voltage at the upper air-dielectric interface, from (1) follows:

$$C = u\left(\frac{\epsilon_0 a_0}{g_2} + \frac{\epsilon_0 a_0}{g_1 + d_1/\epsilon_r}\right)\psi_0^2 + \sum_n^{\infty} \delta_n \psi_n^2 \qquad (9)$$

where

$$\delta_n = \frac{a_0}{2f_n}. \qquad (10)$$

In (9), ψ_n is the nth coefficient of the Fourier expansion of $\psi(x)$ and is given by a formula similar to (3). For $n = 0$ we have:

$$\psi_0 = \frac{1}{a_0}\int_{-a_0/2}^{a_0/2} \psi(x)\, dx. \qquad (11)$$

Again, expression (9) is stationary with respect to the function $\psi(x)$, provided that only variations are considered leaving unchanged the voltage on the conductors. When a trial function is used in place of the true $\psi(x)$, (9) gives an upper bound on the capacitance C. Now if the trial function is chosen in the same way as before, i.e., it is taken as the true voltage distribution for the homogeneous cell of height $2h_0$, the upper and lower bound are typically within a few percent units of each other in a wide range of geometries. Of course, the error could be minimized by giving C a value equal to the average between the upper and lower bound. However, since no practically significant difference is found, the numerical results presented in this paper are based only on lower bound calculations. This has the advantage of a 50-percent saving in computer time. A more rapidly converging series can be obtained from (9) by a procedure similar to that leading from (1) to (7).

A detailed calculation of the trial functions $\rho(x)$,$\psi(x)$ is presented in Appendix A.

III. APPLICATIONS

A. Coupling Capacitance Between Nonadjacent Strips

Let us consider an array of equal and equally spaced strips, as shown in Fig. 3. In Fig. 4 we show the assumed

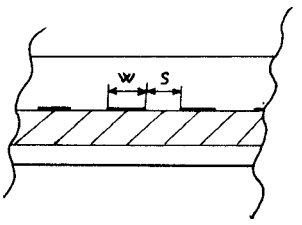

Fig. 3. Uniform array of coupled microstrips.

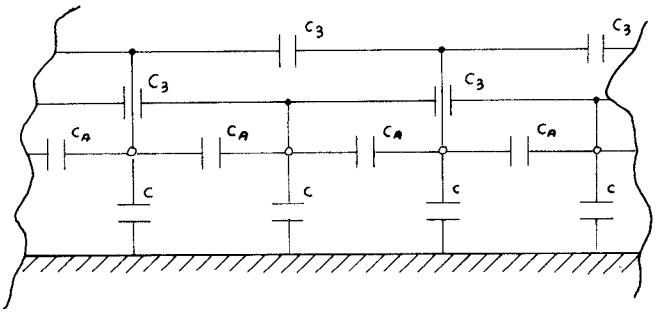

Fig. 4. Capacitance model of the array.

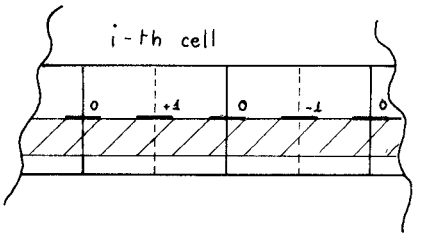

Fig. 5. Array divided into rectangular cells in the presence of a dc excitation.

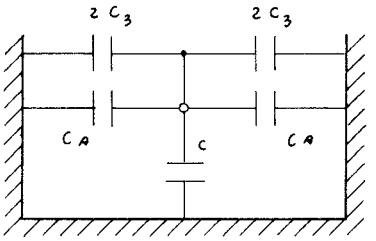

Fig. 6. Capacitance model of each cell.

capacitance model for the array. The self-capacitance C and the coupling capacitance between adjacent strips C_A can be computed by the method described in [1]. A computation procedure for C_3 will now be developed.

Suppose that the strips of the array are held at constant potentials whose values (in volts) are given by the sequence $\cdots 1\ \ 0\ \ -1\ \ 0\ \ 1\ \ 0\ \ -1 \cdots$. If this is the case, the electric-field pattern has an odd symmetry with respect to the center of each grounded strip. Thus electric walls can be introduced without perturbing the electric field (see Fig. 5), so that the array is divided into cells containing only one conductor each. Any one of these cells is a special case of the fundamental cell of Fig. 1, so that its capacitance C_c may be regarded as known. On the other hand, the capacitance model for each cell (drawn from Fig. 4) is as shown in Fig. 6. Thus we have

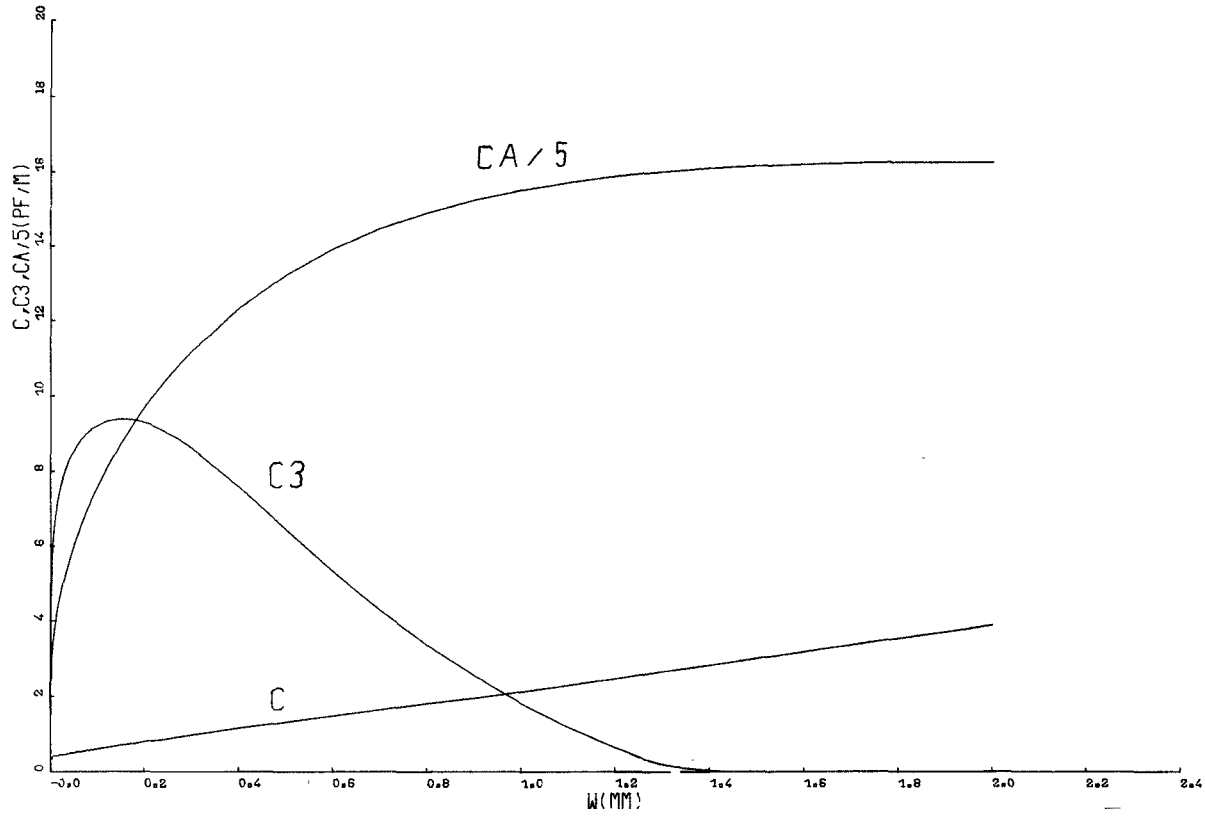

Fig. 7. Capacitance parameters of the array versus strip width.

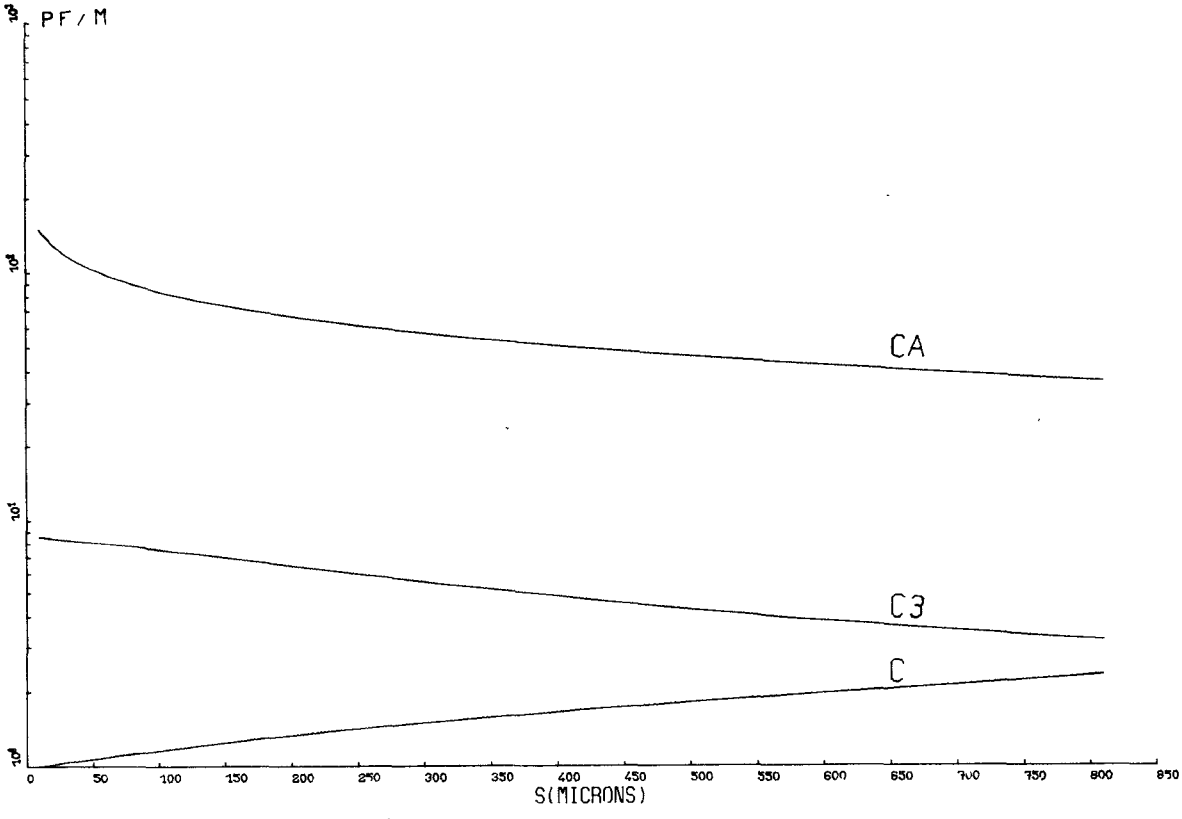

Fig. 8. Capacitance parameters of the array versus strip spacing.

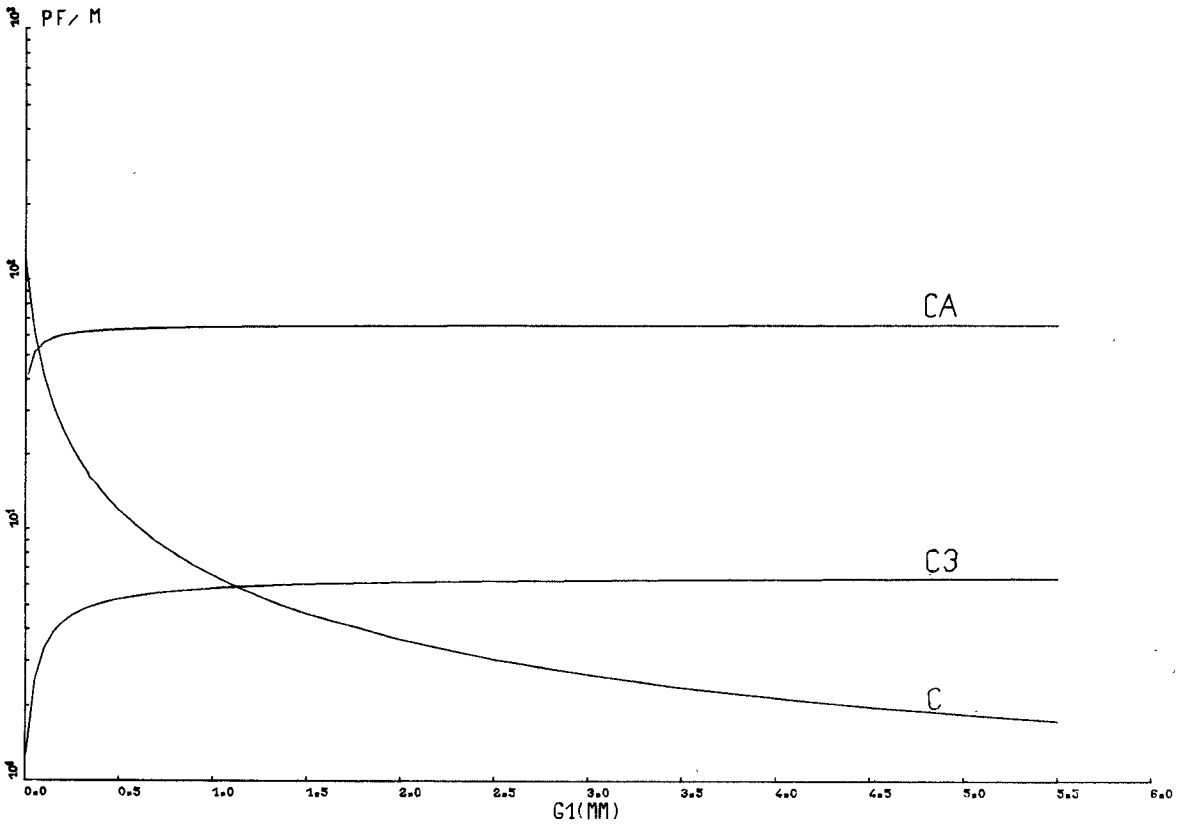

Fig. 9. Capacitance parameters of the array versus lower gap.

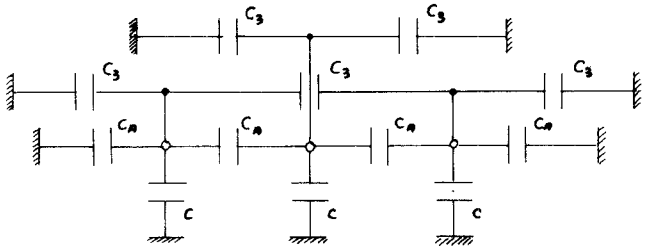

Fig. 10. Capacitance model of three-wire line.

$$C_c = C + 2C_A + 4C_3 \tag{12}$$

yielding C_3 once C_c, C, and C_A have been computed.

As an example, the capacitance model was computed for an array whose reference dimensions are

$$\begin{aligned} g_1 &= g_2 = 10 \text{ mm} \\ d_1 &= 0.5 \text{ mm} \\ s &= 0.2 \text{ mm} \\ w &= 0.5 \text{ mm} \\ \epsilon_r &= 10. \end{aligned} \tag{13}$$

In Figs. 7–9, C, C_A, and C_3 are plotted versus w, s, and g_1, respectively. The parameters which are not varied in each plot are held to the values given by (13). These plots were drawn by a Benson plotter driven offline by a CDC 6600 computer.

It can be seen that C_3 is always small with respect to C_A, while it may be comparable and even large with respect to C depending on the geometry. However, the effect of C_3 on the electrical behavior of the device is usually negligible, owing to the fact that $C_3 \ll C_A$. As a check of this statement, consider the three-wire line that can be obtained from the array by grounding all of the strips, except for three consecutive ones. The capacitance matrix of such a line is

$$\begin{bmatrix} C + 2C_A + 2C_3 & -C_A & -C_3 \\ -C_A & C + 2C_A + 2C_3 & -C_A \\ -C_3 & -C_A & C + 2C_A + 2C_3 \end{bmatrix} \tag{14}$$

as can be inferred from the model of Fig. 10. In the case

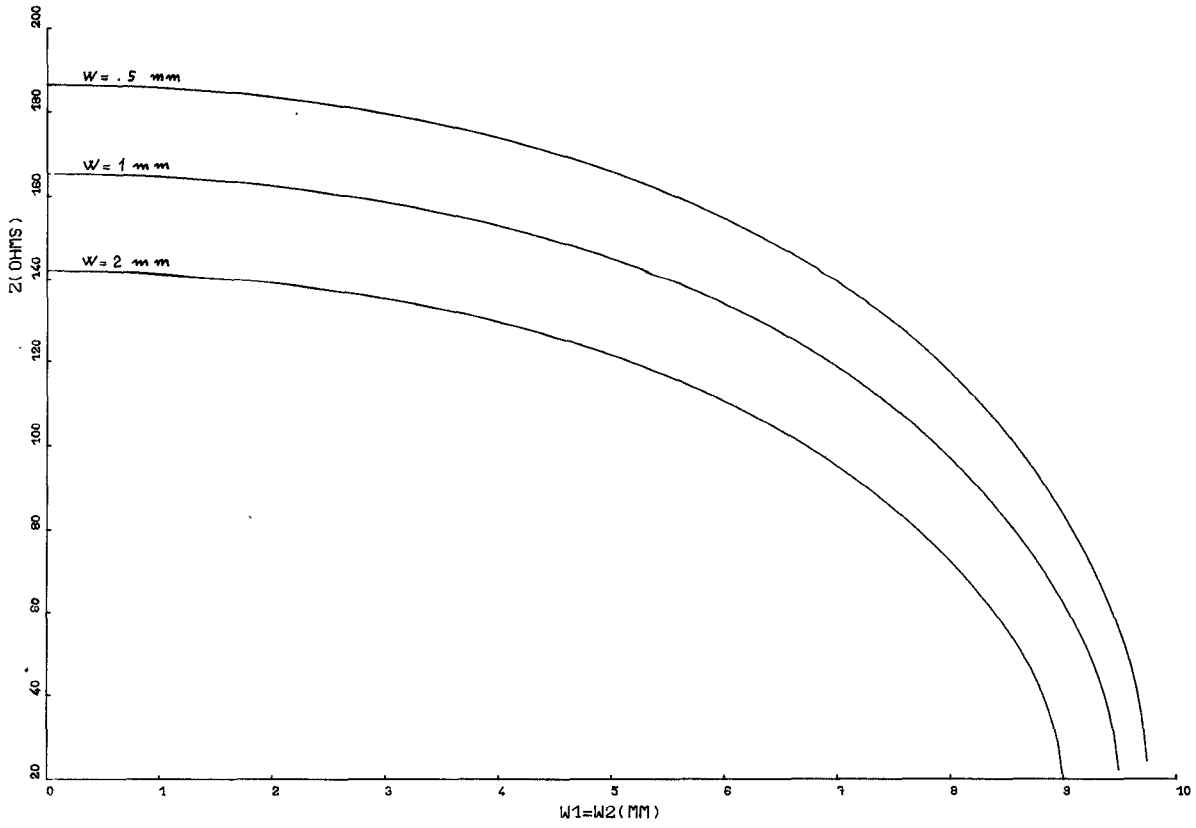

Fig. 11. Characteristic impedance of coplanar stripline.

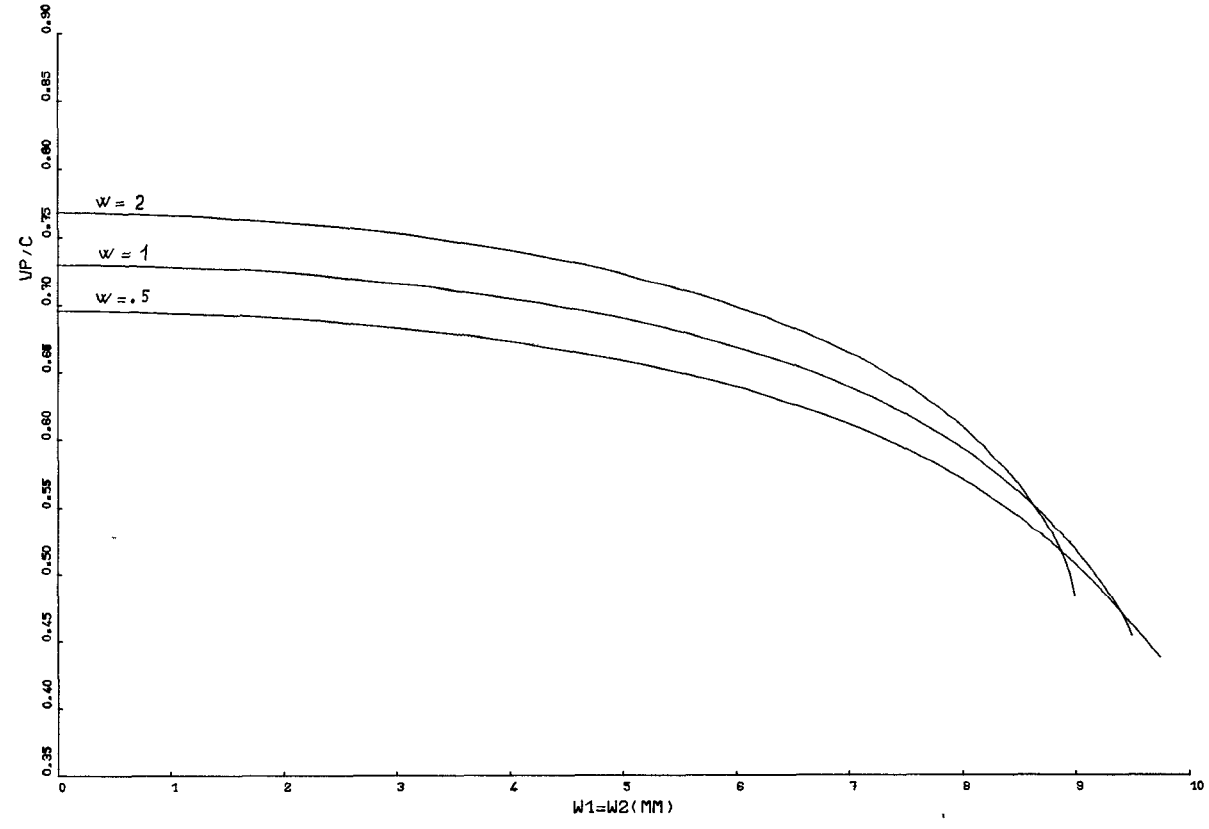

Fig. 12. Relative phase velocity of coplanar stripline.

of the array defined by (13), we have:

$$\begin{bmatrix} 146.24 & -66.02 & -6.44 \\ -66.02 & 146.24 & -66.02 \\ -6.44 & -66.02 & 146.24 \end{bmatrix} \tag{15}$$

while neglecting the effect of C_3 yields:

$$\begin{bmatrix} 133.36 & -66.02 & 0 \\ -66.02 & 133.36 & -66.02 \\ 0 & -66.02 & 133.36 \end{bmatrix}. \tag{16}$$

All capacitances are expressed in picofarads/meter. In the two cases the relative phase velocities of the normal modes are given by

$C_3 \neq 0$	$C_3 = 0$
0.478	0.469
0.447	0.437
0.434	0.431.

(17)

Thus in this case maximum percentage change is about 2 percent.

B. Coplanar Stripline

When the side walls are both electric, the fundamental cell of Fig. 1 is identical to the cross section of a coplanar stripline (see [5], [6]). The characteristic impedance and relative phase velocity can be computed from the dielectric and air capacitances C and C_1 by means of the well-known formulas:

$$Z_c = \frac{1}{v_o(CC_1)^{1/2}}$$

$$v_p = \left(\frac{C_1}{C}\right)^{1/2} \tag{18}$$

where $v_o = 2.998$ m/s. Note that unsymmetrical as well as symmetrical strips may be computed in this way.

In Figs. 11 and 12 the characteristic impedance and relative phase velocity are plotted versus the width $w_1 = w_2$ of the grounded side strips for a coplanar stripline having:

$$\begin{aligned} g_1 &= g_2 = 10 \text{ mm} \\ d_1 &= 0.5 \text{ mm} \\ a_0 &= 20 \text{ mm} \\ \epsilon_r &= 10 \end{aligned} \tag{19}$$

and for three different widths, i.e., 0.5, 1, and 2 mm.

An excellent agreement exists between the data in Figs. 14 and 15 and the results published in [10].

C. Broad-Side Coupled Coplanar Striplines

Fig. 13 shows the cross section of a pair of broad-side coupled coplanar striplines. In this case the section is

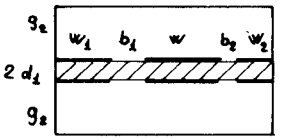

Fig. 13. A pair of broad-side coupled coplanar lines.

Fig. 14. Even- and odd-mode lines for coplanar pair.

symmetrical with respect to the middle of the dielectric slab. In Fig. 14(a) and (b) the associated even and odd cells are shown. Note that the capacitance of the odd cell can be directly computed by the procedure of Section II since this is a special case of the fundamental cell. The capacitance of the even cell may still be computed by the series (7) with [4]:

$$f_n = \frac{a_0}{n\pi\epsilon_0} \cdot \frac{\tanh\,(n\pi g_2/a_0)}{1 + \epsilon_r \tanh\,(n\pi d_1/a_0) \tanh\,(n\pi g_2/a_0)}$$

$$h_0 = g_2. \tag{20}$$

This procedure holds even for cross sections that do not have a vertical plane of symmetry. Once the even and odd capacitances C_e, C_o and the corresponding values in air, C_{e1}, C_{o1}, have been found, the even- and odd-mode impedance and relative phase velocity are given by

$$Z_e = \frac{1}{v_o(C_eC_{e1})^{1/2}}$$

$$Z_o = \frac{1}{v_o(C_oC_{o1})^{1/2}}$$

$$v_{pe} = \left(\frac{C_{e1}}{C_e}\right)^{1/2}$$

$$v_{po} = \left(\frac{C_{o1}}{C_o}\right)^{1/2}. \tag{21}$$

As an example, in Fig. 15 the impedances and phase velocities are plotted as a function of $w_1 = w_2$ for a line having

$$\begin{aligned} g_2 &= 5 \text{ mm} \\ d_1 &= 0.5 \text{ mm} \\ w &= 0.5 \text{ mm} \\ a_0 &= 20 \text{ mm} \\ \epsilon_r &= 10. \end{aligned} \tag{22}$$

Perhaps the most attracting feature of this kind of line is the tight coupling that can be achieved between the two parallel conductors. Let us consider a section of length l of the line as a four-port network, the ports being taken

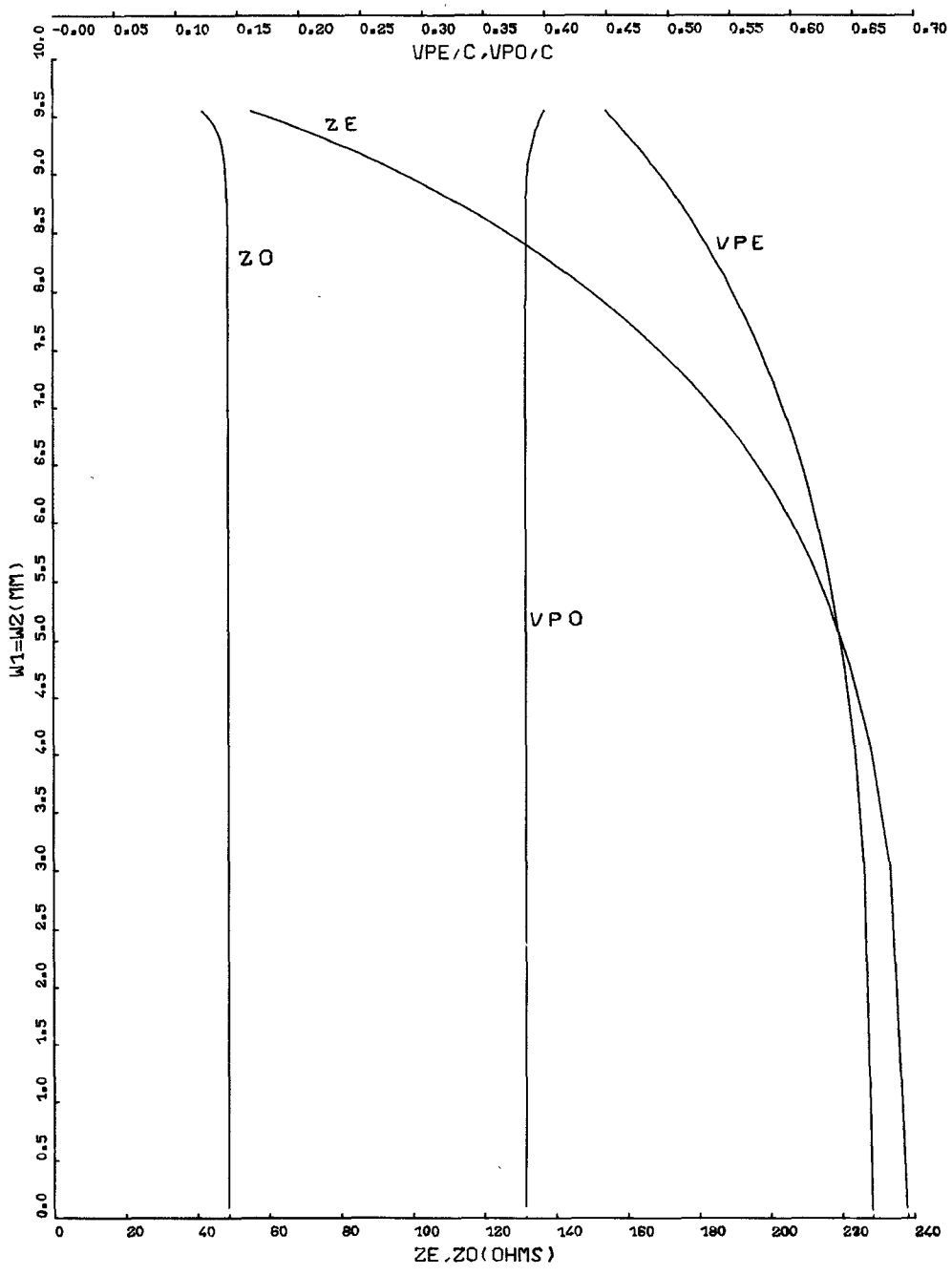

Fig. 15. Even- and odd-mode characteristic impedance and relative phase velocity for coupled coplanar striplines.

in the order shown in the insert of Fig. 16. The entries of the scattering matrix of this network will be denoted by $s_{11},s_{21},s_{31},s_{41}$. Let the load impedance at each of the ports be given by

$$R = (Z_eZ_o)^{1/2}. \tag{23}$$

In order that the device behave as a directional coupler, one of the following sets of conditions must hold:

$$s_{11} = 0$$
$$s_{41} = 0 \tag{24}$$

or

$$s_{11} = 0$$
$$s_{21} = 0. \tag{25}$$

The conditions (24) are met at a given frequency f when the length of the coupler is [7]:

$$l = \frac{v_{pe}v_{po}}{(v_{pe} - v_{po})f}. \tag{26}$$

In this case the coupling in decibels is

$$C = -20 \log_{10} | s_{31} |$$
$$= 20 \log_{10} \left| \frac{1 - \rho^2\theta^2}{\rho(\theta^2 - 1)} \right| \tag{27}$$

where

$$\rho = \frac{(Z_0)^{1/2} - (Z_e)^{1/2}}{(Z_0)^{1/2} + (Z_e)^{1/2}} \tag{28}$$

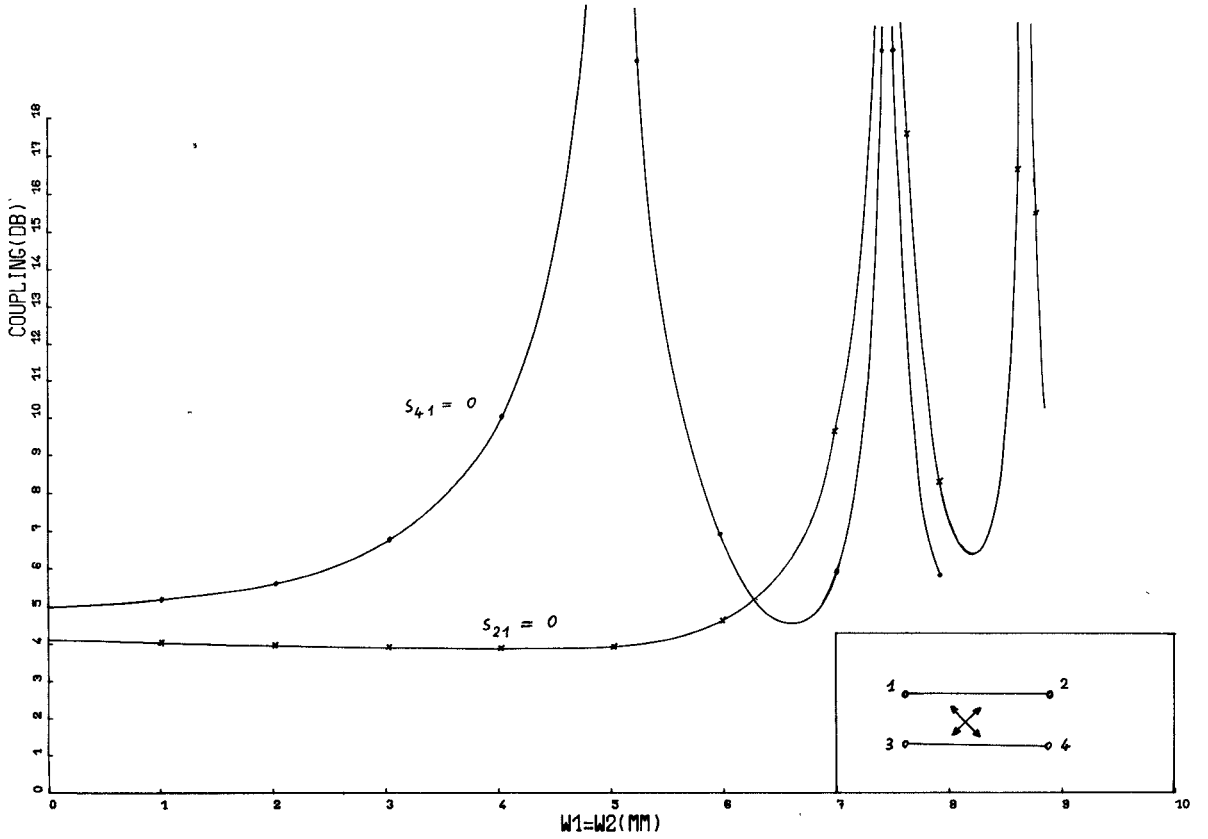

Fig. 16. Coupling in decibels for coplanar stripline directional coupler.

$$\theta = \exp\left(-j\frac{2\pi v_{po}}{v_{pe} - v_{po}}\right). \tag{29}$$

In turn, the conditions (25) are met when the length is one-half of (26). In the latter case the coupling is again given by (27) with (29) replaced by

$$\theta = \exp\left(-j\frac{\pi v_{po}}{vp_e - vp_o}\right). \tag{30}$$

In Fig. 16 the coupling in decibels for these situations is plotted as a function of $w_1 = w_2$ for the same line that is referred to in Fig. 15. As a first example, a 6-dB coupler having $s_{41} = 0$ can be obtained when $w_1 = w_2 = 2.6$ mm with a length of the coupled section of 6.9 cm at 4 GHz. As a further example, a 0-dB coupler from port 1 to 4 can be realized when $w_1 = w_2 = 7.5$ mm with a length of the coupled section of 4.35 cm at 4 GHz.

IV. CONCLUSION

A very general variational procedure has been proposed for the calculation of uniform microstrip transmission lines under the quasi-TEM assumption. This method is highly efficient from a numerical point of view and its formulation is particularly suitable for programming on a digital computer.

A Fortran routine based on the formulas presented here has been written by the author and the results of some calculations are presented. These results agree with other published results concerning the classical cases of uniform microstrip arrays [1] and symmetrical broad-side coupled strips [8].

In addition, other cases such as nonsymmetrical cross sections, coplanar striplines, and coupling between nonadjacent strips may be treated without further complication.

APPENDIX A

GENERAL CONFORMAL MAPPING FOR A RECTANGULAR REGION

Let us consider a rectangular region filled with a homgeneous medium of permittivity ϵ whose boundary is made of two electric and two magnetic walls. A possible geometry is shown in Fig. 17. We want to compute the capacitance $\bar{C}$ between the electric conductors and the line charge density on them when they are held at 1-V and 0-V potentials, respectively. This problem is very general and includes all the cases which are of interest here.

The dimensions of the rectangular cell are denoted by a_0 and h_0. Note that the point $(0,h_0)$ may be assumed to belong to an electric conductor owing to the type of fundamental cells we are interested in (see Fig. 1). The contour of Fig. 17 will be mapped onto that of Fig. 18, whose capacitance is known, by a conformal mapping $p = p(z)$. The mapping is accomplished by successive steps.

First, the contour of Fig. 19(a) is obtained by the mapping function

$$t = \mathrm{sn}\,(Rz,K) \tag{A1}$$

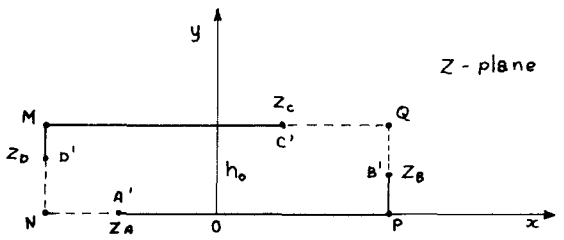

Fig. 17. Rectangular region with electric and magnetic boundaries.

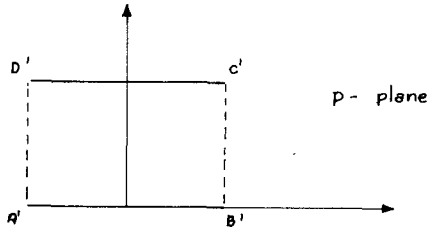

Fig. 18. Final mapping contour.

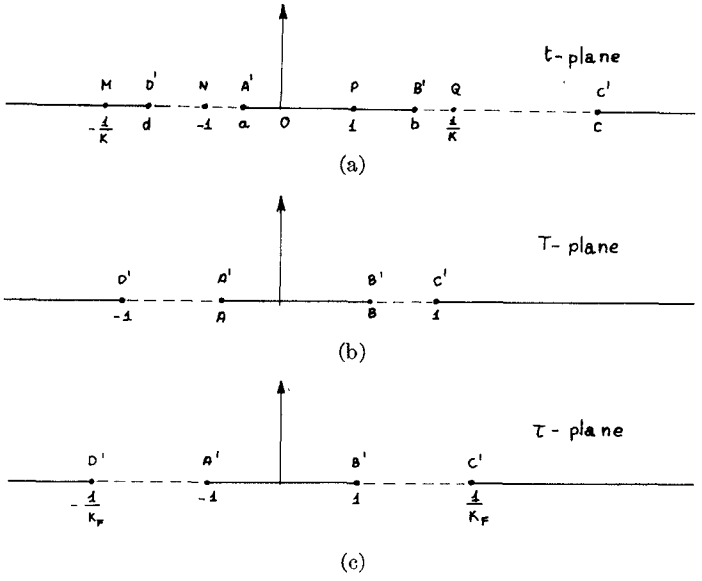

Fig. 19. Intermediate mapping steps.

where sn is the Jacobian sine-amplitude function, and R is given by

$$R = \frac{2F(1,K)}{a_0} = \frac{F[1,(1-K^2)^{1/2}]}{h_0}. \tag{A2}$$

By $F(t,K)$ we denote the first incomplete elliptic integral of modulus K. The constant $K(0 < K < 1)$ is the solution of the transcendental equation

$$\frac{F(1,K)}{F[1,(1-K^2)^{1/2}]} = \frac{a_0}{2h_0} = r \tag{A3}$$

and thus may be expressed in terms of θ functions [3] as follows:

$$K = \left(\frac{\theta_2[0,\exp(-\pi/r)]}{\theta_3[0,\exp(-\pi/r)]}\right)^2. \tag{A4}$$

The real numbers a,b,c,d defined in Fig. 19(a) are now given by (see Fig. 17):

$$\begin{aligned} a &= \mathrm{sn}\,(Rz_A,K) \\ b &= \mathrm{sn}\,(Rz_B,K) \\ c &= \mathrm{sn}\,(Rz_C,K) \\ d &= \mathrm{sn}\,(Rz_D,K) \end{aligned} \tag{A5}$$

while the mappings leading from the contour of Fig. 19(a) to that of Fig. 18 through Fig. 19(b) and (c) are

$$\begin{aligned} T &= \frac{2t}{c-d} - \frac{c+d}{c-d} \\ \tau &= q_1 \frac{T-q_2}{T-q_3} \\ p &= F(\tau,K_F). \end{aligned} \tag{A6}$$

The constants appearing in (A6) must be given the following values:

$$\begin{aligned} q_3 &= \frac{1}{q_2} = \frac{1+AB+[(1-A^2)(1-B^2)]^{1/2}}{A+B} \\ q_1 &= \frac{q_3-A}{q_2-A} \\ K_F &= \frac{B(1-A^2)^{1/2} - A(1-B^2)^{1/2}}{(1-A^2)^{1/2} + (1-B^2)^{1/2}}. \end{aligned} \tag{A7}$$

Finally, A and B are defined in Fig. 19(b) and may be expressed through the first of (A6) as

$$\begin{aligned} A &= \frac{2a}{c-d} - \frac{c+d}{c-d} \\ B &= \frac{2b}{c-d} - \frac{c+d}{c-d}. \end{aligned} \tag{A8}$$

Note that from (A7) and (A8) follows

$$0 < K_F < 1 \tag{A9}$$

so that the last of (A6) is meaningful.

From Fig. 18 the required capacitance $\bar{C}$ can be readily obtained:

$$\bar{C} = \epsilon \frac{A'B'}{C'D'} = 2\epsilon \frac{F(1,K_F)}{F[1,(1-K_F^2)^{1/2}]}. \tag{A10}$$

The charge density $\bar{\rho}(z)$ may be expressed as

$$\bar{\rho}(z) = \pm \left| \frac{d\bar{Q}}{dz} \right| \tag{A11}$$

where the "plus" sign holds for the positive conductor and the "minus" sign for the grounded one. Equation (A11) may be rewritten as

$$\bar{\rho}(z) = \pm \left| \frac{d\bar{Q}}{dp} \frac{dp}{d\tau} \frac{d\tau}{dT} \frac{dT}{dt} \frac{dt}{dz} \right|. \tag{A12}$$

Since the voltage is equal to 1 V, we have

$$\left|\frac{d\bar{Q}}{dp}\right| = \rho_p = \frac{\bar{Q}}{A'B'} = \frac{\bar{C}}{A'B'} = \frac{\epsilon}{F[1,(1-K_F^2)^{1/2}]}. \quad \text{(A13)}$$

Finally, from (A12) and (A13) by means of (A1) and (A5) we obtain

$$\bar{\rho}(z) = \pm\rho_p RH \frac{c-d}{2}\left(\frac{[\mathrm{sn}^2(Rz,K)-1][K^2\,\mathrm{sn}^2(Rz,K)-1]}{[\mathrm{sn}(Rz,K)-a][\mathrm{sn}(Rz,K)-b][\mathrm{sn}(Rz,K)-c][\mathrm{sn}(Rz,K)-d]}\right)^{1/2} \quad \text{(A14)}$$

where

$$H = \frac{(1-A^2)^{1/2}+(1-B^2)^{1/2}}{[(1-A)(1-B)]^{1/2}+[(1+A)(1+B)]^{1/2}}. \quad \text{(A15)}$$

For every z belonging to the boundary φ of the rectangular region shown in Fig. 17, the function sn is real and given by [3]:

$$\mathrm{sn}(R(x+jy),K)_{x+jy\epsilon\varphi} = \frac{\mathrm{sn}(Rx,K)\{1-\mathrm{sn}^2[Ry,(1-K^2)^{1/2}]+K^2\,\mathrm{sn}^2[Ry,(1-K^2)^{1/2}]\}}{1-\mathrm{sn}^2[Ry,(1-K^2)^{1/2}]+K^2\,\mathrm{sn}^2(Rx,K)\cdot\mathrm{sn}^2[Ry,(1-K^2)^{1/2}]}. \quad \text{(A16)}$$

Thus the expression (22) always yields real values for $\rho(z)$. Note that the charge density has a square-root singularity in each of the points A',B',C',D', and is zero in M,N,P,Q.

For upper bound calculations the expression of the voltage $\psi(z)$ on the boundary of the rectangular region (Fig. 17) is required. Since the voltage on the electric walls is constant (equal to 1 V and 0 V, respectively), only the voltage on the magnetic walls needs to be evaluated. In the p plane we have at once (see Fig. 18)

$$\psi_p(p) = 1 - \frac{\mathrm{Im}(p)}{B'C'} = 1 - \frac{\mathrm{Im}(p)}{F(1,(1-K_F^2)^{1/2})} \quad \text{(A17)}$$

where Im denotes the imaginary part. By the use of the expression for Im $(F(\tau,K_F))$ that can be obtained from [3], (A17) gives

$$\psi(z) = \left.\frac{F[(1-K_F^2\tau^2/1-K_F^2)^{1/2},(1-K_F^2)^{1/2}]}{F[1,(1-K_F^2)^{1/2}]}\right|_{\tau=\tau(z)}. \quad \text{(A18)}$$

In (A18), τ is understood to be expressed as a function of z by means of (A6) and (A1). Again, real values are obtained for ψ in every point on the boundary thanks to (A16).

Now let us go back to the cell of Fig. 2 whose capacitance C_o and charge distribution $\rho(x)$ are required. This cell is symmetrical with respect to the x axis so that only one-half of it, say the shaded region in Fig. 2, needs to be considered. The sections of the x axis which are not occupied by conductors may be replaced by magnetic walls. As a consequence, the half-cell is a special case of the general rectangular cell that was studied in the first part of this section. Thus once the parameters z_A,z_B,z_C,z_D have been related to the geometry of the fundamental cell of Fig. 1, (A10) and (A14) can be used to compute C_o and $\rho(x)$ as

$$C_o = 2\bar{C}$$
$$\rho(x) = 2\bar{\rho}(x). \quad \text{(A19)}$$

The second part of (A19) can be put into (3) to compute the coefficients ρ_n. The integral (3) is best evaluated by changing the variable of integration according to:

$$t = \mathrm{sn}(Rx,K).$$

Making use of (A14), we obtain from (3):

$$\rho_n = 2\rho_p H \frac{c-d}{a_0}\int_{-1}^{1}\frac{s(t)g(n,t)}{[(t-a)(t-b)(t-c)(t-d)]^{1/2}}\,dt \quad \text{(A20)}$$

where

$$g(n,t) = \sin\left(\frac{n\pi}{Rl}F(t,K)+n\phi+\theta\right) \quad \text{(A21)}$$

and $s(t)$ is the piecewise-constant function defined in Fig. 20. Thus the right side of (A20) can be evaluated as the sum of three contributions, corresponding to the ranges $(-1,d)$, (a,b), and $(c,1)$ of the variable t. The first and/or the last of these may vanish (when w_1 and/or w_2 do so). Gauss quadrature formulas may be used to remove the singularities from the integrand in much the same way as shown in [2].

A similar procedure is used to evaluate ψ_n by means of (A18). In this case, however, a conventional Simpson integration may be performed since no singularities occur in the integrand.

APPENDIX B

NUMERICAL DETAILS FOR ILL-CONDITIONED CASES

Ill-conditioned cases may occur when the width of the cell a_0 is very large with respect to its height h_0, and the cell is highly asymmetrical. As an example, suppose that

$$w_1 + b_1 + w \ll \tfrac{1}{2}a_0. \quad \text{(B1)}$$

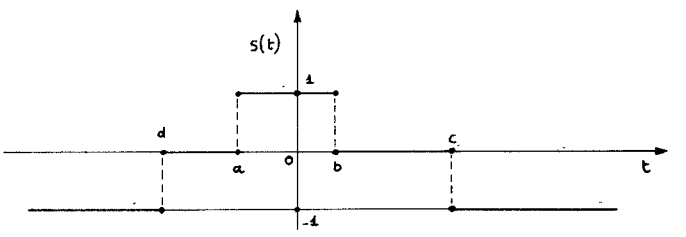

Fig. 20. Step function to be used in integration.

When (B1) holds, the strip is very close to one of the side walls of the cell and is narrow with respect to it.

Now when

$$a_0 \gg h_0 \tag{B2}$$

the solution K to (A3) is very close to 1, so that we have [3]

$$\text{sn}\ (z,K) \simeq \tanh z. \tag{B3}$$

The function $\tanh z$ approaches 1 very quickly as z increases. As a consequence, when (B1) holds together with (B2), the parameters a and b defined by (A5) are very close to -1. If the calculations are implemented on a digital computer capable of m significant digits, when

$$b + 1 < 10^{-m} \tag{B4}$$

a and b will be given the value -1 by the computer and the calculation of K_F (and thus C_o and $\rho(x)$) by (A7) will become impossible.

In order to define exactly the domain of geometries where the difficulty occurs, (B4) is rewritten by means of (A5) as

$$\text{sn}\ [R(-\tfrac{1}{2}a_0 + w_1 + b_1 + w),K] + 1 < 10^{-m}. \tag{B5}$$

(B5) can be easily shown to be equivalent to

$$\frac{w_1 + b_1 + w}{h_0} < \frac{F((\delta)^{1/2},K)}{F(1,(1 - K^2)^{1/2})} \tag{B6}$$

where

$$\delta = \frac{2 - 10^{-m}}{(1 - K^2)10^m + K^2(2 - 10^{-m})}. \tag{B7}$$

For example, when $a_0 = 10\,h_0$ and $m = 6$, (B6) becomes

$$w_1 + b_1 + w < 0.52\,h_0. \tag{B8}$$

Thus the difficulty may arise in cases of pratical interest. When (B6) holds, explicit expressions must be found for the small differences between a, b, and -1. These expressions are then used to compute A, B, and K_F from (A7), (A8).

The basic formula is again found in [3]:

$$\text{sn}\ (-F(1,K) + v,K) = -\left(\frac{1 - \text{sn}^2\ (v,K)}{1 - K^2\ \text{sn}^2\ (v,K)}\right)^{1/2} \tag{B9}$$

where $v < F(1,K)$.

Now if we let

$$\text{sn}\ (-F(1,K) + v,K) = -1 + \epsilon \tag{B10}$$

where $\epsilon \ll 1$, from (B9) we obtain

$$\epsilon \simeq \frac{1 - K^2}{2}\,\frac{\text{sn}^2\ (v,K)}{1 - K^2\ \text{sn}^2\ (v,K)} = \frac{1 - K^2}{2}\,p(v). \tag{B11}$$

Thus when m is large enough, say $m \geqq 6$ (which is almost always the case), and (B6) holds, we have:

$$\begin{aligned} a &\simeq -1 + \tfrac{1}{2}(1 - K^2)\alpha \\ b &\simeq -1 + \tfrac{1}{2}(1 - K^2)\beta \\ d &\simeq -1 + \tfrac{1}{2}(1 - K^2)\Delta \end{aligned} \tag{B12}$$

where

$$\alpha = p\left(\frac{w_1 + b_1}{h_0}\right)$$

$$\beta = p\left(\frac{w_1 + b_1 + w}{h_0}\right)$$

$$\Delta = (2 - I_1)p\left(\frac{w_1}{h_0}\right) + \frac{2(1 - I_1)}{K(1 + K)}. \tag{B13}$$

Here I_1 is the parameter defined in Table I.

From (A8) we obtain

$$A \simeq -1 + (1 - K^2)\,\frac{\alpha - \Delta}{c + 1}$$

$$B \simeq -1 + (1 - K^2)\,\frac{\beta - \Delta}{c + 1} \tag{B14}$$

and from the last of (A7):

$$K_F \simeq \frac{(\beta - \Delta)^{1/2} - (\alpha - \Delta)^{1/2}}{(\beta - \Delta)^{1/2} - (\alpha + \Delta)^{1/2}}. \tag{B15}$$

Equation (B15) is the required formula. In a similar way other ill-conditioned cases may be treated.

REFERENCES

[1] J. I. Smith, "The even- and odd-mode capacitance parameters for coupled lines in suspended substrate," *IEEE Trans. Microwave Theory Tech.*, vol. MTT-19, pp. 424–431, May 1971.

[2] V. Rizzoli, "The calculation of scattering parameters for coupled microstrip arrays of any cross-section," *Alta Freq.*, vol. XLII, pp. 191–199, Apr. 1973.

[3] M. Abramowitz and I. A. Stegun, *Handbook of Mathematical Functions*. New York: Dover, 1965, pp. 569–607.

[4] E. Costamagna, "Fast parameters calculation of the dielectric-supported air-strip transmission line," *IEEE Trans. Microwave Theory Tech.* (Lett.), vol. MTT-21, pp. 155–156, Mar. 1973.

[5] C. P. Wen, "Coplanar waveguide: A surface strip transmission line suitable for nonreciprocal gyromagnetic device applications," *IEEE Trans. Microwave Theory Tech.* (*1969 Symposium Issue*), vol. MTT-17, pp. 1087–1090, Dec. 1969.

[6] T. Hatsuda, "Computation of the characteristics of coplanar-type strip lines by the relaxation method," *IEEE Trans. Microwave Theory Tech.* (Short Papers), vol. MTT-20, pp. 413–416, June 1972.

[7] V. Rizzoli, "Three-wire lines and their use as directional couplers," *Alta Freq.*, vol. XLI, pp. 271–278, Apr. 1972.

[8] D. L. Gish and O. Graham, "Characteristic impedance and phase velocity of a dielectric-supported air strip transmission line with side walls," *IEEE Trans. Microwave Theory Tech.*, vol. MTT-18, pp. 131–148, Mar. 1970.

[9] J. L. Allen and M. F. Estes, "Broadside-coupled strips in a layered dielectric medium," *IEEE Trans. Microwave Theory Tech.*, vol. MTT-20, pp. 662–669, Oct. 1972.

[10] M. E. Davis, E. W. Williams, and A. C. Celestini, "Finite-boundary corrections to the coplanar waveguide analysis," *IEEE Trans. Microwave Theory Tech.* (Short Papers), vol. MTT-21, pp. 594–596, Sept. 1973.